

Antenna-coupled microbolometer based uncooled 2D array and camera for 2D real-time terahertz imaging

F. Simoens^a, J. Meilhan^a, S. Gidon^a, G. Lasfargues^a, J. Lalanne Dera^a, J.L. Ouvrier-Bufferet^a, S. Pocas^a
W. Rabaud^a, F. Guellec^a, B. Dupont^a, S. Martin^a, A.C. Simon^b

^aCEA Leti-MINATEC campus, 17 rue des Martyrs, 38054 Grenoble Cedex 9, France;

^bCEA/DRT/LIST, 91191, Gif/Yvette Cedex – France

(Invited paper)

ABSTRACT

CEA-Leti has developed a monolithic large focal plane array bolometric technology optimized for 2D real-time imaging in the terahertz range. Each pixel consists in a silicon microbolometer coupled to specific antennas and a resonant quarter-wavelength cavity. First prototypes of imaging arrays have been designed and manufactured for optimized sensing in the 1-3.5THz range where THz quantum cascade lasers are delivering high optical power. NEP in the order of 1 pW/sqrt(Hz) has been assessed at 2.5 THz.

This paper reports the steps of this development, starting from the pixel level, to an array associated monolithically to its CMOS ROIC and finally a stand-alone camera. For each step, modeling, technological prototyping and experimental characterizations are presented.

Keywords: Terahertz imaging, Monolithic FPA, Antenna and resonant cavity coupled microbolometer, Uncooled camera

1. INTRODUCTION

As a general rule, many of the terahertz applications that are foreseen would benefit from the availability of a camera with characteristics similar to those of visible digital cameras: compactness, easy-to-use, 2-dimensional (2D) real-time imaging, simplified optics with limited number of moving elements, reliability, low cost in fabrication and operation. Such features would help to spread the use of the THz technology that is still struggling to find the killer application.

2D real-time imaging has first been demonstrated with an indirect conversion of the THz radiation into a visible image through the use of the Pockels' effect [1]. The image was captured in real-time by a commercial CCD camera. To the best of the authors' knowledge, no such camera is currently commercialized. Actually THz video acquisition with a stand-alone camera was first demonstrated in 2005 by the MIT group [2] using a commercial uncooled bolometer IR camera in association with a laser source.

Indeed, in relation to the mentioned criteria, the uncooled bolometer technology is a promising candidate for THz 2D imaging. It operates at room temperature, the arrays are manufactured above advanced CMOS Application-Specific Integrated Circuits (ASICs) in silicon microelectronics foundry, and compact monolithic large 2D arrays –reaching the Mpixel format- are now produced industrially at continuously decreasing prices. The authors' group [3] tested this imaging set-up configuration with Leti-Ulis proprietary amorphous-silicon bolometer sensors [4]. Measurements with a Quantum Cascade Laser (QCL) emitting at 3 THz showed optical absorption efficiency smaller than 0.5%. Even if this sensitivity was sufficient for the tested active THz imaging set-up, these results motivated the study of bolometer pixel architecture specifically tweaked for optimized sensing of THz radiations in order to comply with real-life user-cases.

On the basis of its know-how in such thermal sensors and in sub-millimeter focal plane arrays (FPAs) [5], CEA-Leti has initiated a few years ago the development of fully THz customized bolometer [6]. After a research phase dedicated to model the pixel and to engineer specific technological processes, a complete program has been carried from 2008 till now. This paper reports the steps of this development from the pixel, to an array associated monolithically to a dedicated CMOS ASIC and then to a stand-alone camera. For each steps, modeling, technological prototyping and experimental characterizations are presented.

2. ABOUT IR BOLOMETER MISMATCH FOR THZ SENSING

The standard infrared (IR) bolometer pixel (refer to Figure 1) consists in a micro-bridge architecture where the suspended membrane encompasses the optical absorber and the thermometer layer. The absorber is made of a thin resistive layer that couples to the impinging radiation and induces a heating. This heat is transferred to a thermoresistive layer –Oxyde vanadium for example. The consequent temperature variation is then converted into a resistance change. This resistance change is read-out by a CMOS read-out integrated circuit (ROIC) placed below the membrane. Electrical connection between the resistance and the CMOS upper pads is ensured by thermal insulation legs and vertical studs. A metallic reflector is deposited on the CMOS substrate below each microbridge in order to build a quarter-wavelength cavity between this reflector and the membrane. This sensor element enhances the optical collection efficiency by a factor of 20-30%.

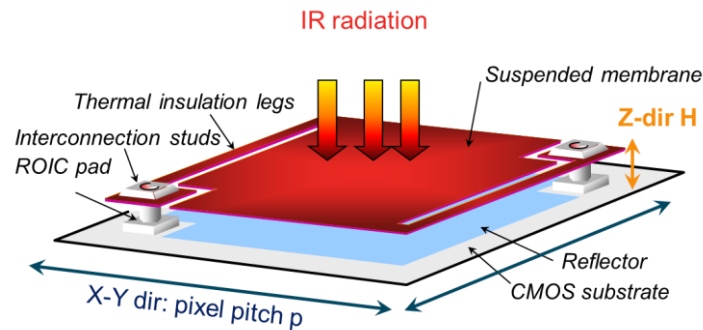


Figure 1. Scheme of a standard IR microbolometer pixel pointing out respectively the Z-direction with the suspended membrane – reflector gap height H and the X-Y directions corresponding to the pixel pitch.

Typically in the Z-direction, the height of the gap between the reflector and the membrane is $H=2 - 2.5 \mu\text{m}$ whilst in the X-Y direction the pixel pitch $p = 17 - 45\mu\text{m}$ is lightly greater than the LWIR wavelength. These dimensions are well matched to the long wavelength IR (LWIR) range defined as $[8 - 14\mu\text{m}]$.

Table 1. Comparison between the standard IR bolometer dimensions and the IR to THz wavelength requirements

	LWIR (8-14μm)	High end >1THz	Low end < 1 THz
Z-dir	$H_{\text{IR}} 2.5 \mu\text{m} = \lambda/4$	$H_{\text{IR}} (2.5\mu\text{m}) \ll \lambda$	$H_{\text{IR}} (2.5\mu\text{m}) \llllll \lambda$
XY-dir	$p \sim 17-45\mu\text{m} > \lambda$	$p \sim \lambda/2$	$p \ll \lambda/2$

This situation rapidly degrades when longer wavelengths are considered. If one considers first THz radiations in the high end range, let's say at frequency above 1THz, then the X-Y dimensions are close to half wavelength, and therefore the absorber can be considered as a patch antenna fairly well matched. Inversely, the Z-dimension is very badly matched to the THz range, by a factor of 40 at 3 THz ! This mismatching is even worse in the low range of the THz spectrum, between 0.1 and 1THz. Both the Z and XY dimensions don't fit the long wavelengths.

This quick analysis emphasizes the 2 main elements that should be tweaked to customize uncooled bolometer arrays for THz detection: the resonant cavity height H and the pixel pitch p . The Japanese company NEC has lightly modified this structure with the deposition of a resistive metallic layer at the top of their microbridge 2-level structure. This modification induces a better optimization of the equivalent impedance in the 3 THz range. But since pixel dimensions are kept unchanged, the Z-dimension is not optimized. Moreover in the low end THz range, the sensitivity quickly degrades.

3. LETI PIXEL: ANTENNA-COUPLED MICROBOLOMETER

3.1 Pixel architecture

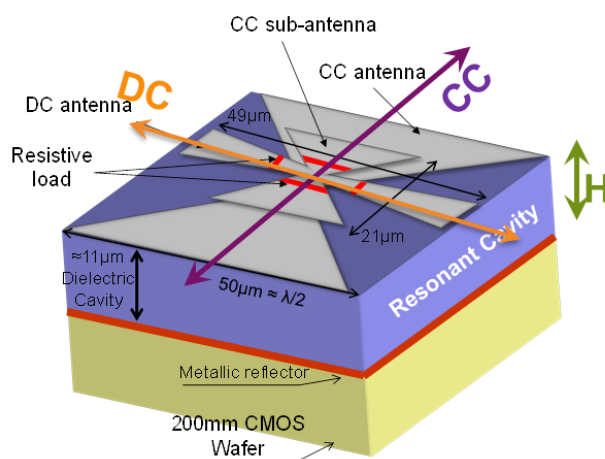


Figure 2. Scheme of the Leti THz microbolometer pixel pointing out 2-storied crossed bow-tied antennas ‘CC’ and ‘DC’, and the thick resonant quarter-wavelength cavity located below the ‘CC’ antenna.

The (patented) Leti pixel architecture (Figure 2) is uniquely characterized by the combination of the following features:

- 1- The THz radiation absorber and the thermometer are separate elements. The optical collection is ensured by crossed bow-tie antennas located above a thick quarter-wavelength cavity matched to THz wavelengths. The thermometer function is provided by a thermo-resistive layer supported by a central microbridge derived from standard IR technology.
- 2- The crossed bow-tie antennas are located at two different Z-direction levels. One polarization is detected by a bow-tie antenna –called CC- deposited onto the CMOS substrate. The surface currents induced by the absorbed radiation are then coupled to metallic planes placed on the microbridge via a capacitive effect. Resistive loads are heated by these currents and consequently produce Joule dissipation in the suspended membrane. For the crossed polarization, a direct coupling ‘DC’ bow-tie antenna with its own resistive loads is located on the membrane. This unique two-storied antenna architecture permits the tuning of the optical coupling of both polarizations independently and with no mutual interferences. This is particularly relevant when unpolarized light is to be detected. Possibly, one of the antenna directions can be removed.
- 3- The antenna-coupled microbridge is built above a metallic reflector that is buried in a thick oxide layer in order to define a quarter-wavelength backplane below the antenna floor.
- 4- The pixels combining the cavity and the microbridge structure are collectively processed above a CMOS ROIC, ending up with a monolithic 2D sensor fully compatible with standard microelectronics silicon technology.
- 5- This monolithic integration is achieved thanks to Through-Oxide-Vias (TOVs) that interconnect electrically the bolometer resistance with the CMOS upper metallic contacts. This technological brick constitutes a major challenge since high and thin diameter TOVs have to be etched and metallized with a high yield.
- 6- Amorphous-silicon is used as thermo-resistive material.

3.2 Simulation results

This pixel structure can be tuned to sense any frequency range provided that the dimensions of the antennas and cavity are adjusted. Extensive work has been carried out to model the electromagnetic (EM) behavior of these thermal imagers [7]. The 2D arrays are considered as infinitely large planar-periodic structures when compared to working frequency range. A pixel is modeled as a Floquet cell with periodic boundaries conditions (refer to the figures of Table 2). The excitation by an incident plane wave is applied at the top of this unit. The underneath silicon wafer layer behaves as an

infinite thick layer (effective thickness more than 20 times larger than wavelength) represented by a 20 μm thick Si box backed by a Perfect Matching Layer (PML).

The modeling of the spectral reponsivity of the pixel has been considered through two approaches.

1. The ‘useful’ spectral absorption efficiency is represented by the ratio between the Joule heating of the membrane and the total impinging optical power onto the pixel that can be expressed as following

$$\eta(f) = \frac{\Sigma P_{\text{absorbed}}}{P_{\text{incident}}} \quad (1)$$

This coupling efficiency can be extracted from 3D EM simulations by integrating the current surface produced in the antenna resistive loads located on the membrane (a of Figure 3) while the incident power corresponds to the power applied at the excitation port.

2. An indirect spectral absorption efficiency can be computed from the spectral reflectivity given by

$$1 - R(f) = 1 - \frac{P_{\text{reflected}}}{P_{\text{incident}}} = 1 - |S_{11}|^2 \quad (2)$$

The scattering matrix S11 value is generally directly available as a 3D code model output (b of Figure 3). On the other hand this quantity overestimates the optical efficiency η(f) since some power absorbed below the excitation port is lost outside the bolometer suspended membrane.

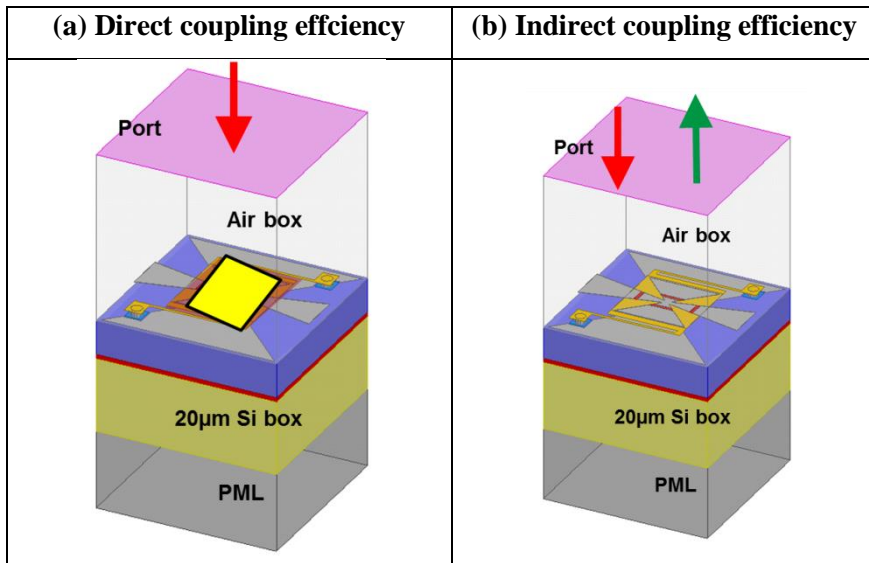


Figure 3. Two approaches considered to model the spectral reponsivity of the unitary pixel integrated within the 2D array

Pixel designs have been optimized at different frequencies [8] with the use of commercial finite-element method simulators like HFSS® or Comsol®.

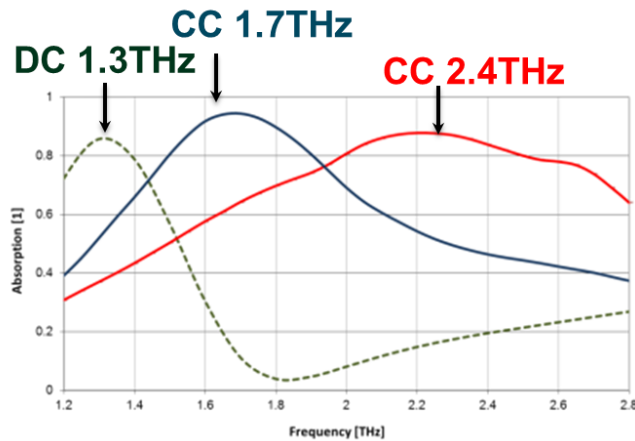


Figure 4. Simulated spectral absorptions of pixel designs optimized for detection above 1 THz.

Two pixels have first been designed for optimum absorption above 1 THz (Figure 4). For both of them, the DC antenna is optimized for maximum absorption at 1.3 THz whereas the ‘CC’ polarization can be detected in the 1.7 THz or 2.4

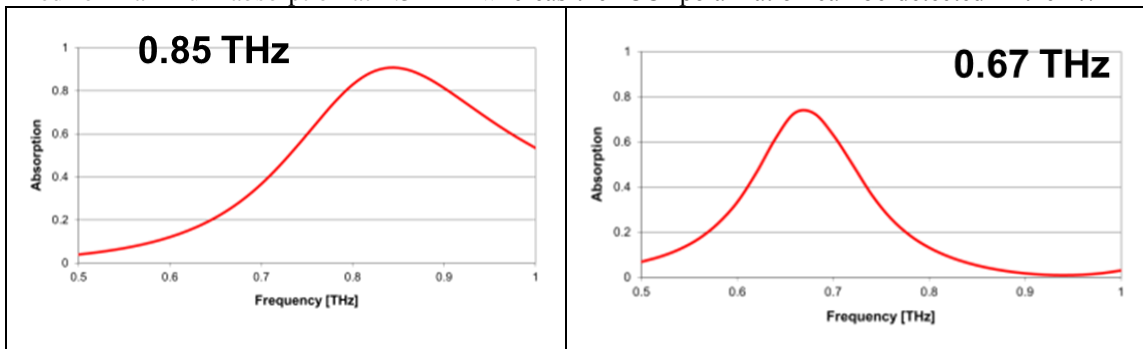


Figure 5. Simulated spectral absorptions of pixel designs optimized for detection below 1 THz in the atmospheric windows centered around 0.85 THz and 0.67 THz.

Two other pixels have been modeled for absorption below 1 THz in the atmospheric windows centered around 0.85 THz and 0.67 THz (Figure 5). The antennas are tailored to match the wavelength while the cavity height is kept unchanged thanks to specific innovative structure changes under patents.

3.3 Experimental tests

FPA's above 1 THz have been manufactured in 160x120 format directly processed above a raw 200 mm Si wafer. 32 pixels of this array were individually accessed by an external ROIC [9]. A specific experimental set-up has been developed in order to generate the spectral responsivity from the interferograms generated by a Fast Fourier Transform (FTS). 2 metrology procedures were studied. The first technique outputs the signal reflected by the array to be compared to the S11 parameter while the second method involves the direct measurement of the bolometer output voltage with a synchronous detection.

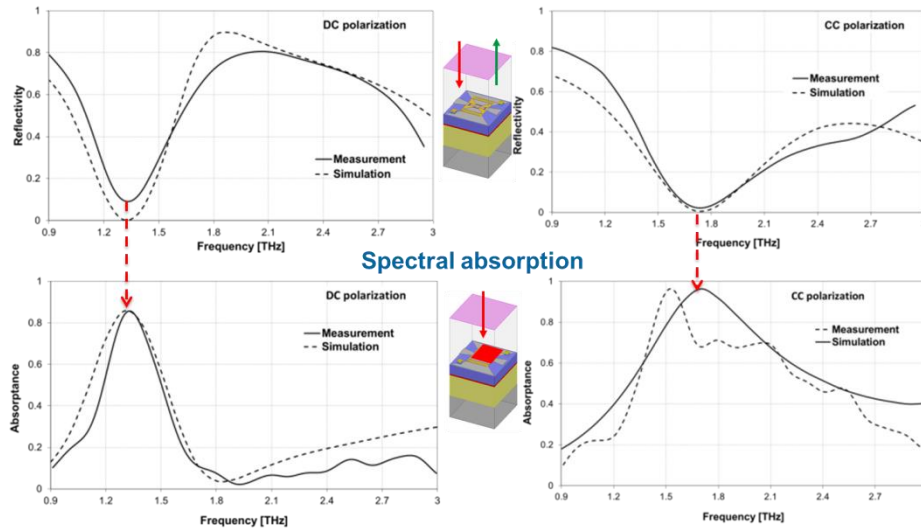


Figure 6. Comparison of spectral reflectances and spectral absorptions of DC and CC antennas extracted from measurements and 3D FEM simulations.

As shown by the Figure 6, good agreement is noted between the empirical and theoretical curves for both polarizations.

4. ARRAY: MONOLITHIC 320X240 PIXEL FPA WITH CMOS READ-OUT

4.1 Design and manufacturing of above-CMOS bolometer array prototypes

On the basis of the above 1 THz designs presented in the section 3, 320x240 bolometer arrays have been processed a dedicated CMOS ASIC. This ROIC is derived from standard LWIR bolometer design. Row-wise reading scheme (Figure 7) allows the integration of the bolometer current during 125 μ s per pixel in the 5 pF capacitance of its associated capacitive trans-impedance amplifier (CTIA). A 25 Hz video rate was targeted.

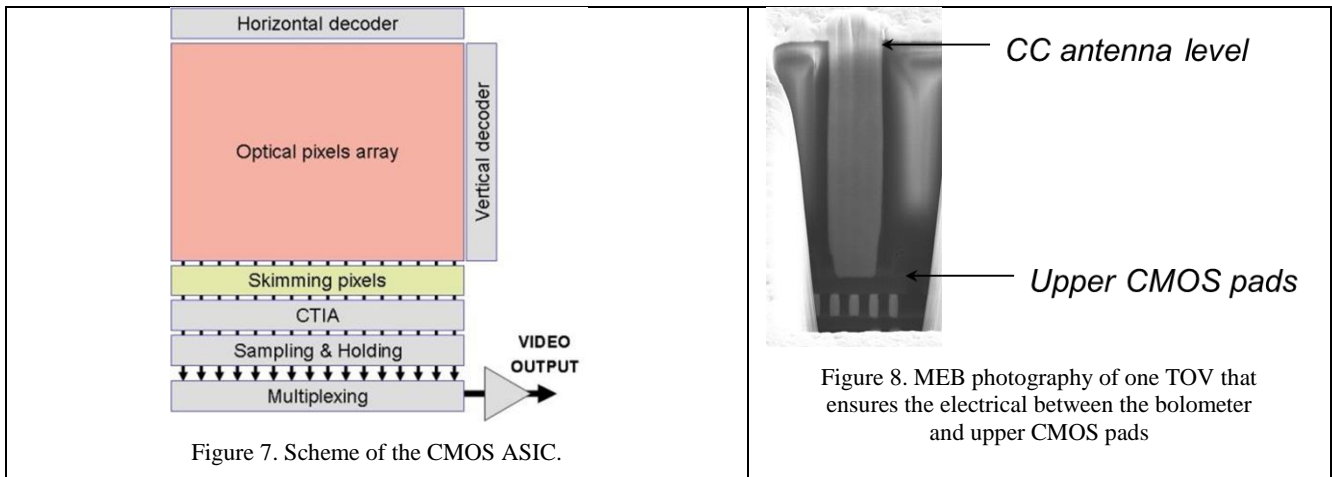


Figure 7. Scheme of the CMOS ASIC.

Figure 8. MEB photography of one TOV that ensures the electrical between the bolometer and upper CMOS pads

As mentioned in the previous section 3, one major technological challenge was to work out a technological flow of the complete stack above the CMOS wafer. In particular the TOVs that ensures the electrical between the bolometer and upper CMOS pads have been successfully manufactured with a high yield: smaller than 1 Ohm resistance has been measured, and more than 99.5% of the 320x240 pixels are functional for 56 out of 63 chips available per 200 mm wafer.

4.2 Real-time imaging laboratory tests

Imaging tests have been carried out in laboratory set-up where samples intercept the collimated beam of a THz QCL delivering an optical beam at 2.5 THz.



Figure 9. Laboratory set-up to image the transmission of a leaf.

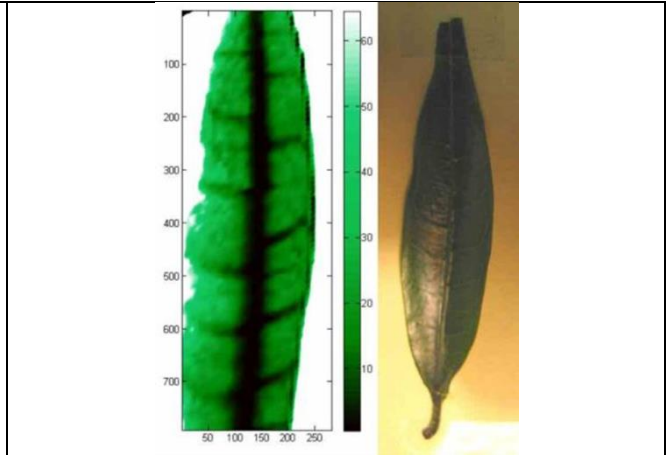


Figure 10. Laboratory set-up to image the transmission of a leaf.

The water concentration of a leaf has been imaged in transmission (Figures 9 and 10). Scissors concealed in an envelop have been imaged in real-time while they were translated through the THz beam delivered by the QCL (Figure 11 and 12).



Figure 11. Scissors that have been concealed in an envelop.

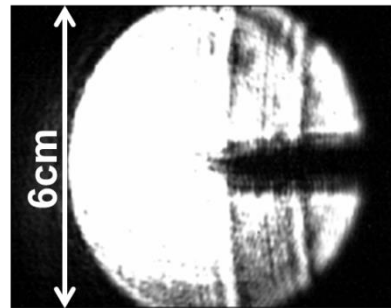


Figure 12. One frame extracted from the video sequence acquired while the envelop was translated through the THz beam.

For these tests, the FPA was housed in a fairly cumbersome laboratory vacuum package and the CMOS –clocks, biases, Analog to digital converter- was driven by a laboratory instrument.

5. CAMERA: REAL-TIME THZ IMAGING STAND-ALONE CAMERA

5.1 Camera integration

Specific efforts have been dedicated to the development of a hand-held stand-alone camera that integrates the THz bolometric chip. It involved the design of a specific vacuum packaging (Figure 13) to house the FPA with an appropriate window than simultaneously transmits the THz radiation and ensures good hermeticity –10⁻³ mbar is targeted. Zeonex® has been used till now, but other materials can be integrated like quartz or High resistivity Silicon.

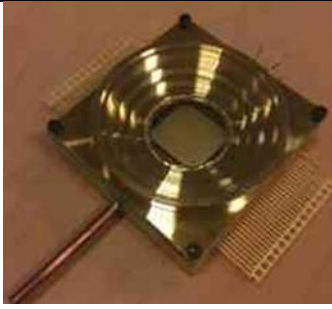


Figure 13. Specific vacuum packaging developed to integrate the bolometer FPA.

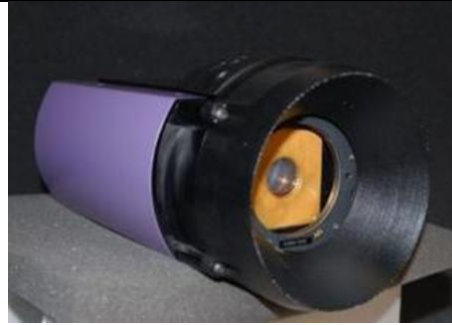


Figure 14. THz camera

A specific front-end electronics made of 2 different cards has also been developed. A first card delivers low-noise analog voltages and digitizes the chip output voltage. The second card, a FPGA board, drives the sensor and ensures synchronization between the camera and external devices. This complete imaging system has been housed in a hand-held stand-alone housing (Figure 14).

5.2 Camera performances

A specific setup has been developed to measure with a high accuracy the camera sensitivity. It combines a QCL emitting at 2.5 THz and a Thomas Keating (TK) Instruments® power-meter [10]. In a general way, no filter is used during these experiments.

Imaging root mean square (RMS) noise that includes the pixel noise and the ROIC and digitizing chain contributions is $400 \mu\text{V}$ RMS. Smallest variation of impinging power that can be detected is calculated as the ratio of RMS noise to the device responsivity. At 2.5 THz the best measured responsivity is 12.6 MV/W for the CC polarization. Hence the best detection power threshold per pixel is equal to 32 pW , placing this camera at state-of-the art of above 1THz uncooled camera. This quantity corresponds to a detection threshold of the array operating in real-time video mode with no filters, no synchronous detection, no pixel binning, neither frame averaging.

5.3 Applied tests of the camera: profiling TDS beam

Two essay campaigns demonstrated sensitive 2D real-time profiling of the beam delivered by 2 different classical Time-Domain Spectrometer (TDS) setups [11]. Even with the first TDS delivering maximum power at 0.4 THz , the beam has been imaged in real-time with a 29 dB SNR at peak [12]. With the second TDS set-up, detected integrated THz power of the source emitting as low as 25 nW has been resolved with sufficient SNR to observe tiny details of the beam shape as shown in Figure 16.

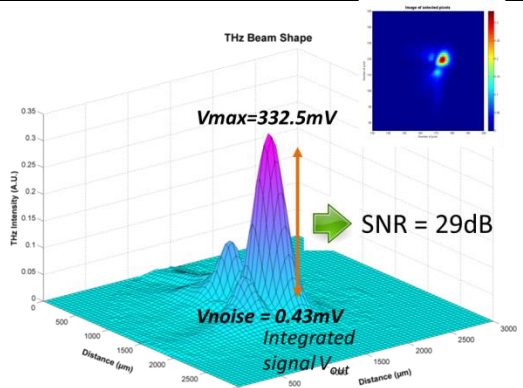


Figure 15. Example of 2D images of the TDS beam extracted from real-time acquisition with lower detected power of 10 nW with a $\text{SNR}=10$ [11]

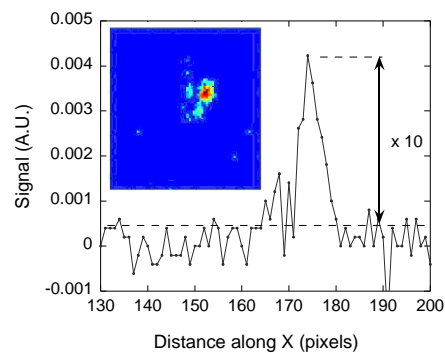


Figure 16. Example of 2D image and cross-section of the TDS beam extracted from real-time acquisition with lower detected power of 10 nW and a $\text{SNR}=10$ [11]

As a conclusion of these tests, even if the tested 320x240 FPAs are optimized for 2 THz center resonance frequencies far from the TDS beam spectrum, significant absorption remains below 1 THz. This capability comes from the ultra-wideband spectral absorption of such THz antenna-cavity coupled bolometers. Such feature would significantly help the scientific groups to align any THz set-up in real time.

5.4 Applied tests of the camera: real-time imaging on a large field of view with a screening portal system demonstrator

A complete reflection active THz imaging demonstrator combining QCLs with the 320x240 THz FPA has been developed [13]. This system images objects or persons located at 1 m from the demonstrator housing with successive illumination of elementary areas of 40x60 mm². A large plane mirror guides the illumination beam towards the scene and then collects the reflected and backscattered beam by the imaged objects. A folded Newton telescope focuses the beam onto the camera. The resulting total optical path from the QCL-based source to the camera is 4 m long, of which 2 meters are in air.

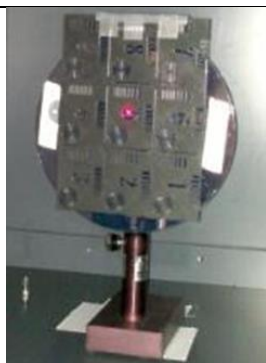


Figure 17. 3x3 metallized patterns set-up. The surface of each pattern is 4x6 cm²

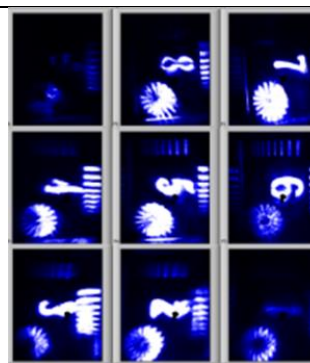


Figure 18. THz image of the 3x3 pattern array surface

Elementary images of objects concealed under clothes have been acquired in real-time with spatial resolution better than 2 mm [14]. Thanks to the equipment of the large plane mirror by rotational motors, the scanning of a large field of view has been tested. 3x3 patterns with metallized painting have been imaged in less than 3 seconds (Figures 17 and 18). Each pattern area corresponds to 4x6 cm², resulting in a 12x18cm² imaged in reflection. The combination of this scanning system and of the real-time camera opens the way to fast scanning of large surface within short time.

CONCLUSION AND PERSPECTIVES

An innovative uncooled technology has been developed with the aim to fulfill the need of affordable, easy-to-use and highly-sensitive detectors for real-time THz imaging.

A monolithic 2D array sensor based on the use of antennas and of a resonant quarter-wavelength cavity has been designed, prototyped and extensively characterized. A good matching between modeling and experimental data has been found for the main figures of merit of these sensors, and in particular the spectral absorption.

Arrays of bolometers monolithically processed above dedicated CMOS ASICs have been designed, manufactured and tested. Thanks to the full compatibility to silicon microelectronics technology, technological barriers have been lifted and high yields have been observed.

320x240 pixel FPA have been integrated in a camera. While the camera was operating in video mode, a NEP better than 30 pW per pixel has been characterized at 2.5 THz. This result places this uncooled sensor at the state-of-the art of such device.

Further technological developments will target performance improvement of the prototyped sensor and the development of an array optimized in the 0.6 – 1 THz range where atmospheric and material transmission are more favorable.

ACKNOWLEDGEMENTS

The authors would like to thank especially the DSNP department for its CEA internal support. We are grateful to all the colleagues that contributed to this work, in particular the University of Savoie, the University of Paris 7, the University of Rennes, the Ecole Normale Supérieure de Paris for their fruitful collaboration.

REFERENCES

- [1] Q. Wu, T.D. Hewitt and X.-C. Zhang, "Two-dimensional electro-optic imaging of THz beams" *Appl. Phys. Lett.* 69, 1026–1028 (1996)
- [2] A.W. Lee and Q. Hu, "Real-time, continuous-wave terahertz imaging by use of a microbolometer focal-plane array" *Optics Letters* 30 (19), 2563-2565 (2005)
- [3] F. Simoens, T. Durand, J. Meilhan, P. Gellie, W. Mainault, C. Sirtori, S. Barbieri, H. Beere and D. Ritchie, "Terahertz imaging with a quantum cascade laser and amorphous-silicon microbolometer array" *Proc. SPIE* 7485, 74850M (2009)
- [4] Yon J.J. et al., "First demonstration of 25 μ m pitch uncooled amorphous silicon microbolometer IRFPA at LETI-LIR" *Proc. SPIE* 5783, 432-440 (2005).
- [5] F. Simoens, P. Agnese, A. Béguin, J. Carcey, J.C. Cigna, J.-L. Pornin, P. Rey, A. Vandeneynde, L. Rodriguez, O. Boulade, J. Lepennec, J. Martignac, E. Doumayrou, V. Reveret and L. Vigroux, "Submillimeter Bolometers Arrays for the PACS/Herschel Spectro-Photometer" *Proc. SPIE* 5498, 177-186 (2004)
- [6] E. Peytavit, P. Agnès, J.L. Ouvrier Buffet, A. Beguin and F. Simoens, "Room Temperature Terahertz Microbolometers" *Proc. of IRMMW-THz*, 257- 258 (2005)
- [7] D.T. Nguyen, F. Simoens, J.L. Ouvrier-Bufferet, J. Meilhan and J.L. Coutaz, "Broadband THz Uncooled Antenna-coupled Microbolometer Array – Electromagnetic Design, Simulations and Measurements" *IEEE Trans. on Terahertz Science and Technology* 99, 1-7 (2012)
- [8] J. Meilhan, F. Simoens, J.L. Lalanne-Dera, S. Gidon, G. Lasfargues, S. Pocas, D.T. Nguyen, J.L. Ouvrier-Bufferet, "Terahertz frequency agility of uncooled antenna-coupled micro-bolometer arrays" *Proc. IRMMW-THz*, 1-2 (2012)
- [9] F. Simoens, J. Meilhan, S. Pocas, J.L. Ouvrier-Bufferet, T. Maillou, P. Gellie, S. Barbieri, "THz uncooled microbolometer array development for active imaging and spectroscopy applications" *Proc. of IEEE IRMMW-THz*, 1-2 (2010)
- [10] J. Meilhan, B. Dupont V. Goudon, G. Lasfargues, J.L. Lalanne Dera, D.T. Nguyen, J.L. Ouvrier-Bufferet, S. Pocas, T. Maillou, O. Cathabard, S. Barbieri, F. Simoens, "Active THz imaging and explosive detection with uncooled antenna-coupled microbolometer arrays" *Proc. SPIE* 8023 (1), 80230E–80230E–13 (2011)
- [11] J. Meilhan, J. Oden, P. Cavalié, S. Dillhon, J.-F. Roux, J.L. Coutaz, J. Tignon. and F. Simoens, "Room-temperature video-rate imaging of terahertz pulses generated by femtosecond lasers using an array of microbolometers" *Int. Workshop OTST2013*, (2013)
- [12] J. Oden, J. Meilhan, J. Lalanne-Dera, J.-F. Roux, F. Garet, J.L. Coutaz, F. Simoens, "Imaging of broadband terahertz beams using an array of antenna-coupled microbolometers operating at room temperature". *Optics Express* 2013 (21), 4: 4817-4825 (2013)
- [13] F. Simoens, J. Meilhan, J.L. Lalanne-Dera, S. Gidon, G. Lasfargues, S. Pocas, J.L. Ouvrier-Bufferet, D. Guillaume, V. Jagtap, S. Barbieri, "Complete THz system for reflection real-time imaging with uncooled antenna-coupled bolometer arrays" *IEEE IRMMW-THz2012*, 1-2 (2012)
- [14] F. Simoens, J. Meilhan, "Terahertz real-time imaging uncooled array based on antenna and cavity coupled bolometers", approved for publication in *Philosophical Transactions A* (2013)